A multi-plateaus contact model for rough surfaces

G. F. Wang*, X. M. Liang and D. Yan

Department of Engineering Mechanics, SVL, Xi'an Jiaotong University, Xi'an 710049, China

* E-mail: wanggf@mail.xjtu.edu.cn

Abstract: The accurate calculation of real contact area between rough surfaces is a key issue in tribology. In this paper, based on the geometrical information of total contact area and the number of contact spots with respect to surface separation, a new method is proposed to determine the relation between real contact area and normal load. The contact of rough surfaces is treated as an accumulation of incremental multi-plateaus indentations with varying average contact radius. Comparisons with direct finite element calculations and some other theoretical predictions demonstrate the efficiency of this approach.

Key words: Contact, Rough Surfaces, Plateaus, Real Contact Area

1. Introduction

Contact of rough surfaces has aroused wide attention since the beginning of last century owing to the thriving developments in railways, gears, bearings, etc. It has been long aware that separations exist between contact surfaces, and the real contact area is only a small portion of the nominal contact area. Because of its intimate relation with friction, wear, lubrication and sealing, an accurate prediction of real contact area becomes a critical important issue in tribology.

Early in 1957, Archard [1] modelled rough surface as spherical protuberances covered with even smaller spheres, and predicted a power-law relationship between external load and real contact area. Greenwood and Williamson [2] (GW model) described asperities by spheres with an identical radius and a Gaussian distribution of their heights, and found an approximately linear relationship between load and real contact area. Furthermore, Bush et al. [3] (BGT model) developed a more general model, which treated asperities as paraboloids and described the joint distribution of heights and curvatures by random process [4]. Assuming the size of contact spots following a power law distribution, Majumdar and Bhushan [5] presented a contact model (MB model) on account of the fractal nature of rough surfaces. Using the concept of magnification, Persson [6] derived a general theory of contact mechanics for randomly rough surfaces, in which the power spectral density (PSD) of rough surfaces is required.

Developments in measuring instruments such as profilometer, interferometer and AFM allow precise observation of micro- and nano-scale roughness and improve our

knowledge in rough topographies. A typical rough profile of grinding surface measured by a white-light interferometer is shown in Fig. 1. In fact, the variations in height are much smaller than the characteristic length in the horizontal direction. Moreover, stepped structures were observed even down to nano-scale by AFM [7]. Therefore, it seems more appropriate to describe asperities on rough surfaces by plateaus rather than by smoothly spherical surfaces.

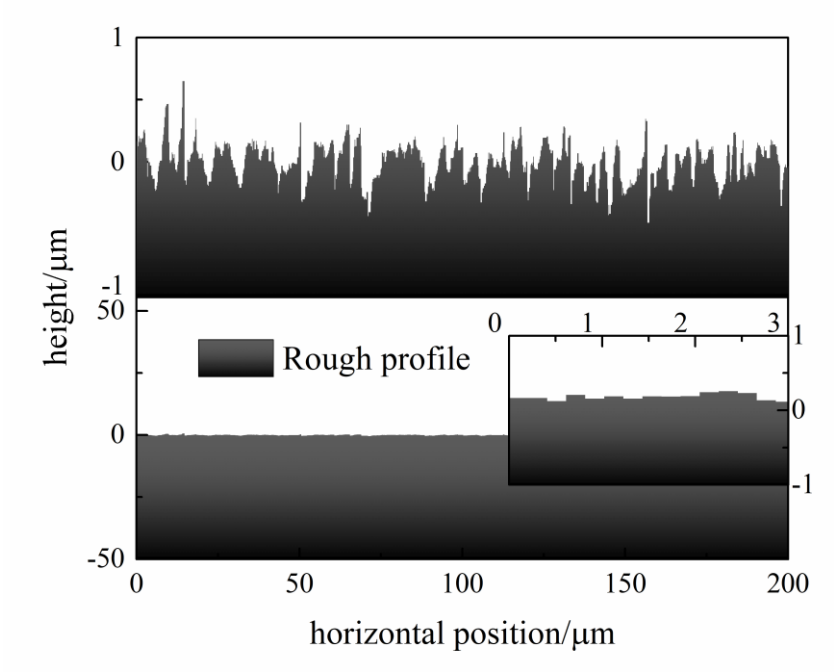

Figure 1. A typical rough profile of grinding surface in different scales

It is noteworthy that the indentation by a rigid sphere can be approximated by the superposition of indentation by circular punches of varying radii [8, 9]. This concept can be employed to deal with contact of rough surfaces. In this study, we present a multi-plateaus model for elastic contact between rough surfaces. At any specified surface separation, protuberances on rough surfaces are modelled as a pile of flat-ended cylinders. The average radius of these cylinders is estimated from the total contact area and the number of contact spots. Then, based on the elastic solution of a

flat punch [10], the increased load with respect to a small variation of separation can be obtained. By accumulation of such response, the relationship between normal load and real contact area can be established. For two numerical generated rough surfaces and an actual grinding surface, our theoretical model gives fairly good agreements with direct FEM simulations.

2. The multi-plateaus contact model

Consider the contact between a rigid plane and an elastic substrate with rough surface as shown in Fig. 2a. The rigid plane is pushed by a load P approaching the rough surface parallel its mean plane. The mean plane of rough surface is chosen as a reference plane to locate the position of the rigid plane by z, named as surface separation.

To describe the topography of rough surface, a set of virtual planes are adopted to cut the rough surface. At a surface separation z, the virtual plane generates cross sections of irregular geometries, as shown in Fig. 2b. The amount of contact spots and the total area of cross sections are functions of z as $N(z)$ and $A_c(z)$, respectively. These two functions can characterize the topography of rough surfaces to some extent, which can be obtained from geometrical analysis if the rough topography is known. For example, the area $A_c(z)$ can be extracted from the Abbot-Firestone curve [11]. Though the area $A_c(z)$ of cross sections is obtained from purely geometrical analysis, we treat it as real contact area and try to determine the load P required to achieve such real contact area. It should be pointed out that surface separation is an intermedium

variable to relate or synchronize the contact area and the number of contact spots, which is different from the compressive depth.

At a specified separation z, the contact response of the rough surface is simplified by N identical flat-ended cylinders with an average radius R, which possess the same total contact area $A_c(z)$, as shown in Fig. 2c. Thus the contact radius R is given by

$$N(z)\pi R(z)^2 = A_c(z) \tag{1}$$

For a decrement dz of surface separation, the incremental load dP can be obtained according to the Sneddon's solution as [10],

$$\mathrm{d}P = 2E^* R(z) N(z) \mathrm{d}z \tag{2}$$

E^* represents the composite elastic module and is related to the Young's modulus E and the Poisson's ratio ν of the elastic substrate as $E^* = E/(1-\nu^2)$.

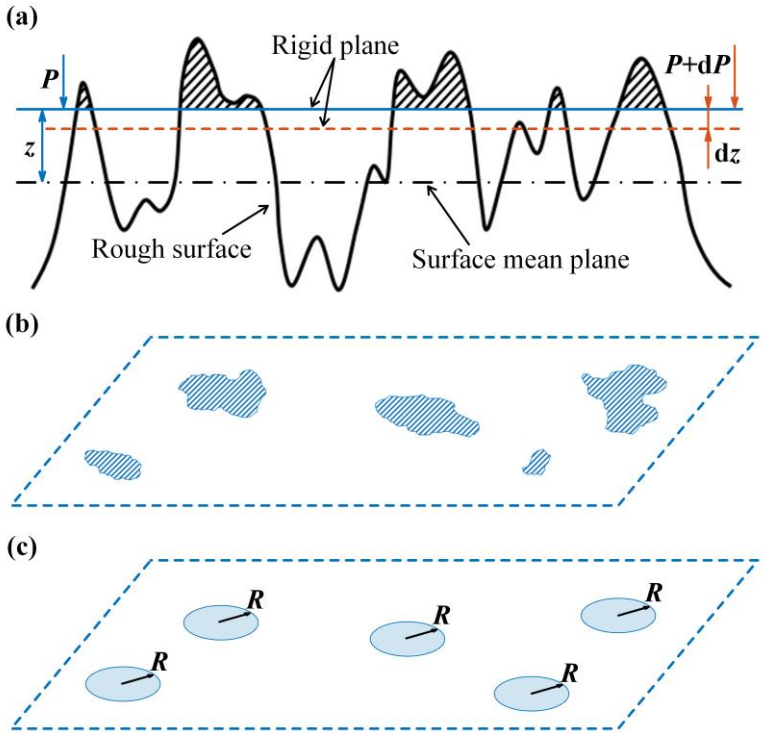

Figure 2. A schematic diagram of the multi-plateaus model

Therefore, for a compression with the surface separation decreasing from infinity to z, the load P is determined by integration of Eq. (2). Combining Eq. (1) and Eq. (2) gives the load as

$$P(z)=\frac{2E^*}{\sqrt{\pi}}\int_z^{\infty}\left[A_c(z)N(z)\right]^{1/2}\mathrm{d}z \tag{3}$$

In addition to the function of $A_c(z)$, the load and the contact area at any surface separation can be determined, then the relationship between load P and contact area A_c can be established.

3. Finite element simulation

To test the efficiency of our model, finite element simulations are performed on contact of various rough surfaces by using the commercial software ABAQUS. An

analytical rigid plane is brought into contact against an elastic substrate with rough surface, as shown in Fig. 3. The Young's module E of the substrate is 100 GPa and its Poisson's ratio ν is 0.3. The nominal length L_x and the width L_y of the rough surface are both 200 μm, and the height of the substrate is 50 μm.

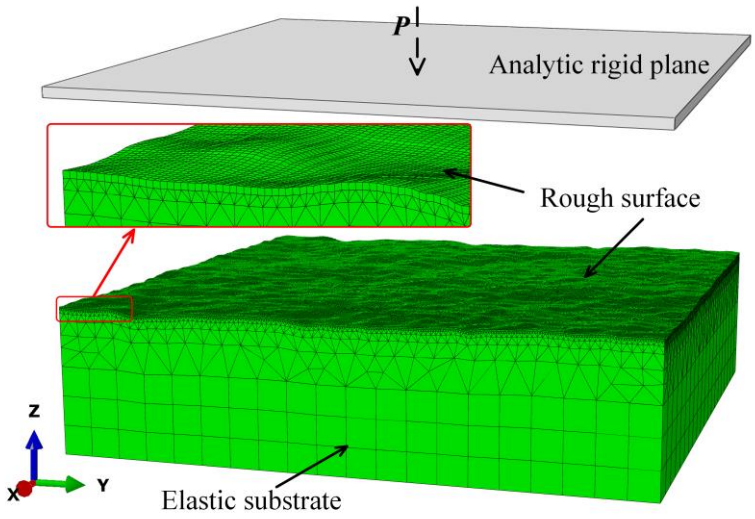

Figure 3. Finite element models of the rough surface contact

To produce artificial topographies of rough surfaces, a square grid with identical spacing is generated on the upper surface of the substrate, with 256 nodes along both the x-axis and y-axis. Hence, the lateral resolution of rough surfaces is 0.781 μm. The heights of these nodes are generated randomly through an open source code in MATLAB [12]. Moreover, the lower frequency cutoff and the upper frequency cutoff are incorporated through a slight modification. The heights of these nodes can also be assigned from actual rough topographies.

In our finite element simulations, eight-node linear hexahedral (C3D8I) elements and ten-node quadratic tetrahedral (C3D10) elements are adopted to discretize the substrate, in which the meshes are gradually coarsened along the z-axis from top to

bottom, as shown in Fig. 3. The amount of elements in simulation is 334992. Frictionless is assumed on the contact interface. For each rough surface, convergence test has been performed to ensure the accuracy of computational results.

4. Results and discussions

Two typical isotropic rough surfaces in engineering are generated from power spectral density, and their PSD and topographies are shown in Fig. 4 and Fig. 5. The details of these two surfaces are listed in Table 1, in which σ is the root-mean-square roughness, H is the Hurst exponent, q_0, q_s and q_r are the lower frequency cutoff, the upper frequency cutoff and the roll-off wavevector, respectively. Surface A in Fig. 4 is self-affine fractal on all length scale. While a roll-off frequency is introduced for surface B in Fig. 5 to truncate its PSD into two parts. The moments of these two surfaces are also calculated as given in Table 2, which will be used in some theoretical models.

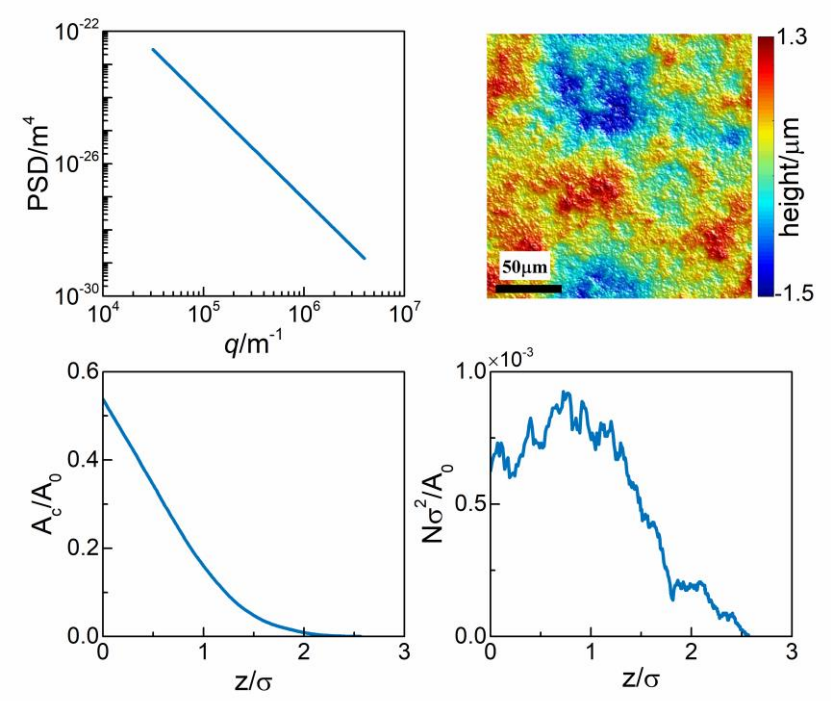

Figure 4. Surface A: (a) PSD, (b) topography, (c) A_c/A_0 and (d) $N\sigma^2/A_0$

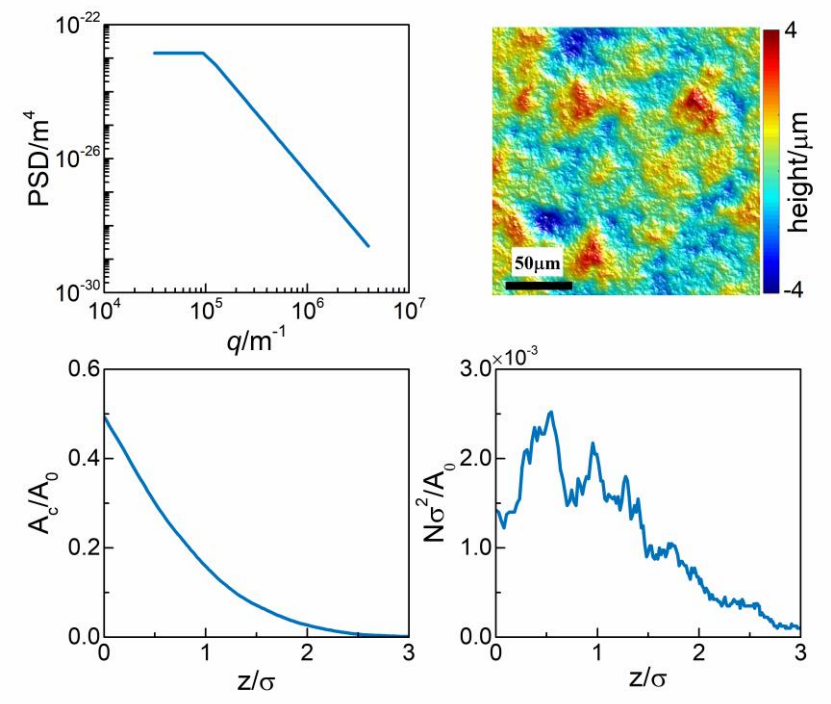

Figure 5. Surface B: (a) PSD, (b) topography, (c) A_c/A_0 and (d) $N\sigma^2/A_0$

Table 1. Parameters for generating surface A and surface B

Surface	σ/μm	H	q_0/m^{-1}	q_r/m^{-1}	q_s/m^{-1}

A	0.5	0.5	3.14e4	3.14e4	4.02e6
B	1.0	0.8	3.14e4	1.00e5	3.00e6

Table 2. Moments of the PSDs of surface A and surface B

Surface	$m_0(\sigma^2)/\mu m^2$	m_2	$m_4/\mu m^{-2}$
A	0.250	0.0110	0.0446
B	1.00	0.0391	0.0992

In our contact model, the contact area and the number of contact spots are required as presented in section 2. With the height information of discrete nodes on the rough surfaces, a numerical program is coded to calculate the contact area and the contact spots with respect to surface separation. The increment of surface separation is chosen as 0.002 times the height of the highest node. A_c normalized by the nominal area A_0 and N normalized by A_0/σ^2 of surfaces A and B are displayed in Fig. 4 and Fig. 5, respectively. As the surface separation decreasing, the contact area A_c generally increases, while the number of contact spots may change irregularly. Then using Eq. (3), one can predict the contact response of these rough surfaces through numerical integration, as given in Fig. 6 and Fig. 7.

For comparisons, the load-area relations predicted by BGT model [3], Persson's theory [6] and an improved GW model by McCool [12] are also included in Fig. 6 and Fig. 7, which can be derived by using the moments of PSD in Table 2. The finite element results are chosen as a standard to test these theoretical models. For an

objective comparison, all models have shared the same topographic information of rough surfaces.

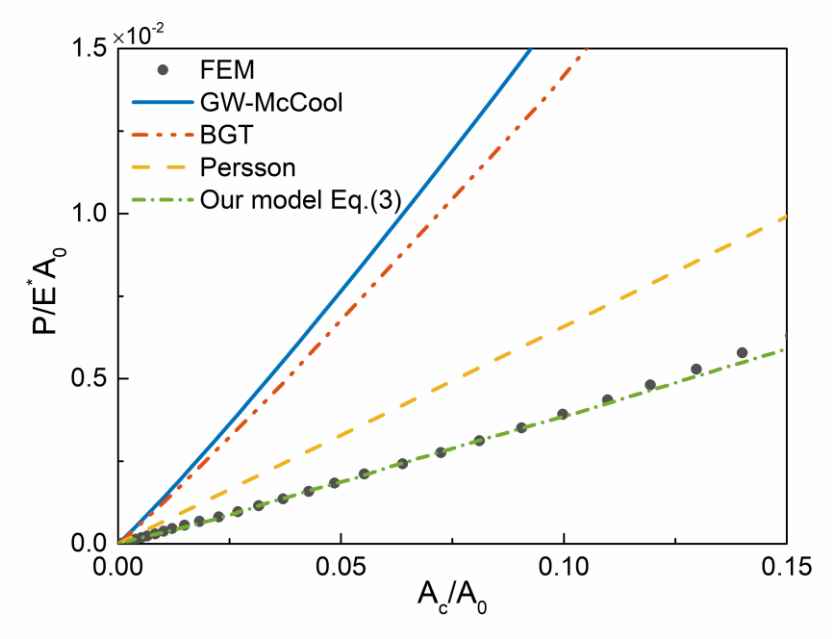

Figure 6. Dimensionless load P/E^*A_0 as a function of the contact area fraction A_c/A_0 for surface A

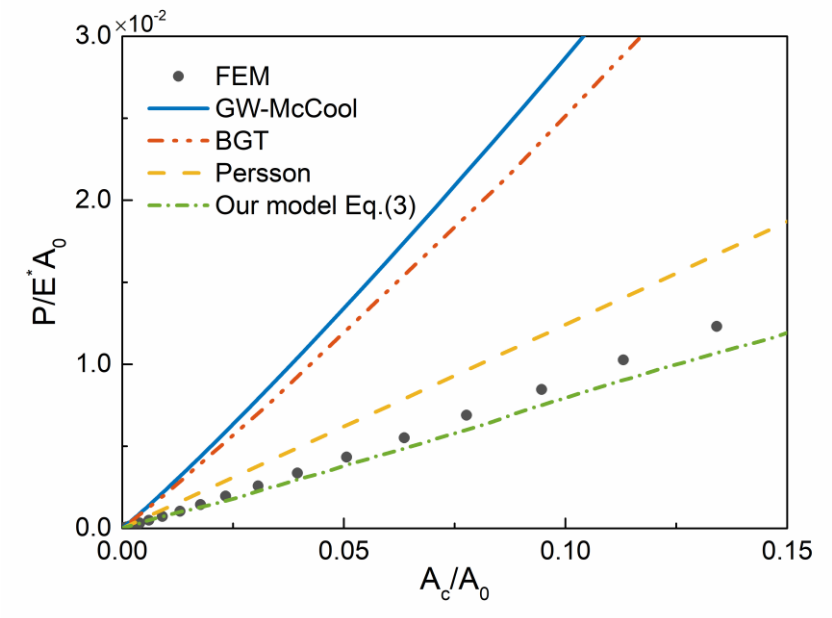

Figure 7. Dimensionless load P/E^*A_0 as a function of the contact area fraction A_c/A_0 for surface B

For two typical rough surfaces, it is seen from Figs. 6 and 7 that these theoretical models predict approximately linear dependency between normal load and real contact area, while different proportionalities are predicted. From large to small, the proportionalities predicted by theoretical models are sorted by the improved GW model, BGT model, and then Persson's model. However, all these theoretical models predict a larger proportionality than the finite element result. It implies that, to achieve a given real contact area, the required load will be overestimated by these theoretical models. Instead, it is found that the new proposed model agrees fairly well with finite element result.

A real machined grinding surface is also considered. The size of this surface is 52.2×52.2 μm^2, and its topography is measured by a white-light interferometer as shown in Fig. 8. 256×256 data are collected on the height information, resulting in a lateral resolution of 0.204 μm. This grinding surface displays evidently anisotropic features, and its PSDs in the x- and y-direction are distinct clearly. The root-mean-square roughness σ of this surface is 0.103 μm. For such non-Gaussian and anisotropic rough surface, it is difficult to use the existing theoretical models to calculate the real contact area. However, the new proposed model is not confined by these conditions at all. The contact area and the contact number are calculated with the development of surface separation, as shown in Fig. 8. Then the load-area relation is determined and plotted in Fig. 9, which displays reasonable agreement with finite element simulation again.

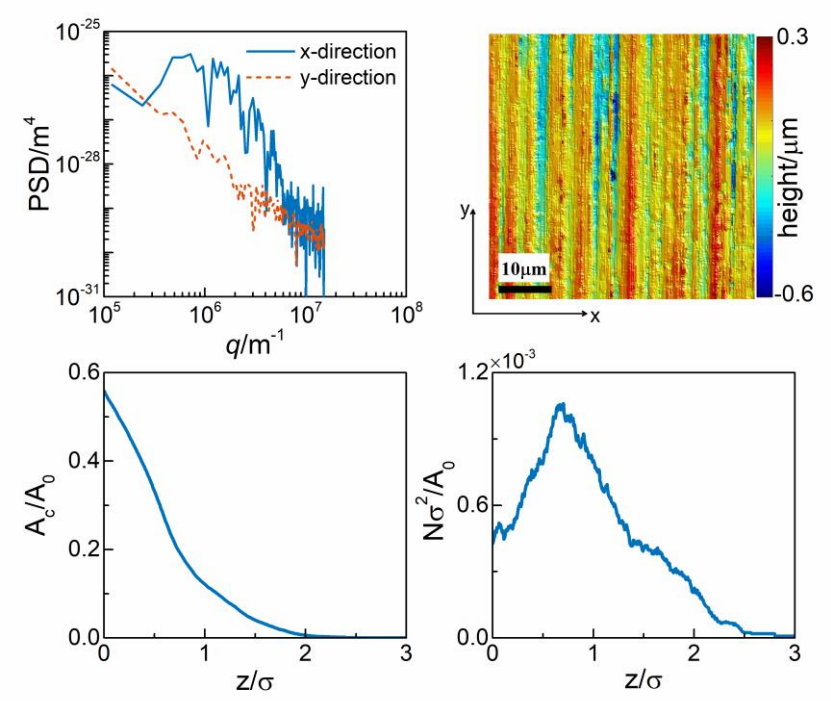

Figure 8. Grinding surface: (a) PSD, (b) topography, (c) A_c/A_0 and (d) $N\sigma^2/A_0$

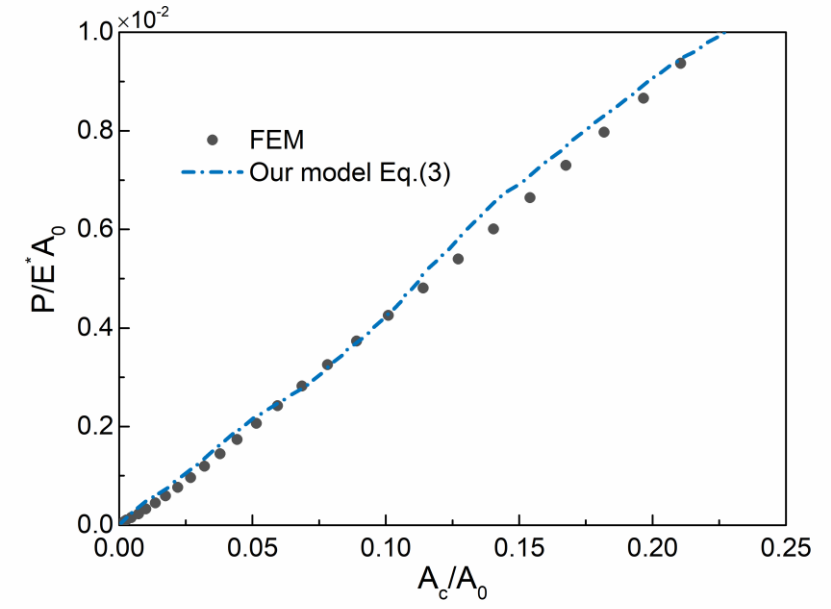

Figure 9. Dimensionless load P/E^*A_0 as a function of the contact area fraction A_c/A_0 for grinding surface

Through the analysis of three typical rough surfaces, it is proved that the new advanced model is not only accurate but also has wider applicability. Moreover, the

new model is quite convenient to be conducted through only simple geometrical analysis of rough surfaces. It should be acknowledged that in present model only elastic deformation is considered and the interaction between asperities is also neglected, which may be considered in future work.

5. Conclusions

By using the total contact area and the number of contact spots with respect to surface separation, which can be obtained through geometrical analysis of surface topographies, a multi-plateaus contact method is proposed to determine the relation between real contact area and load. At any decrement of surface separation, the contact of rough surfaces is modeled by a group of flat-ended cylinders with a varying average radius, and the overall response is achieved by such accumulation. For some typical rough surfaces, the present model gives fairly good agreements with direct finite element simulations, compared to other theoretical models. This work provides a simple and efficient approach to calculate the real contact area of rough surfaces.

Acknowledgements

G.F.W. proposed the contact model, X.M.L. conducted the theoretical analysis, and D.Y. performed the finite element simulation. G.F.W. and X.M.L. prepared the manuscript. Supports from the National Natural Science Foundation of China (Grant No. 11525209) are acknowledged.

References

[1] Archard, J. F. (1957). Elastic Deformation and the Laws of Friction. Proceedings of the Royal Society A-Mathematical, Physical and Engineering Sciences, 243(1233), 190–205.

[2] Greenwood, J. A., & Williamson, J. B. P. (1966). Contact of Nominally Flat Surfaces. Proceedings of the Royal Society A-Mathematical, Physical and Engineering Sciences, 295(1442), 300–319.

[3] Bush, A. W., Gibson, R. D., & Thomas, T. R. (1975). The Elastic Contact of a Rough Surface. Wear, 35(1), 87–111.

[4] Nayak, P. R. (1971). Random Process Model of Rough Surfaces. Journal of Lubrication Technology, 93(3), 398–407.

[5] Majumdar, A., & Bhushan, B. (1991). Fractal Model of Elastic-Plastic Contact Between Rough Surfaces. Journal of Tribology, 113(1), 1-11.

[6] Persson, B. N. J. (2001). Theory of Rubber Friction and Contact Mechanics. Journal of Chemical Physics, 115(8), 3840-3861.

[7] Qu, M. N., Xu, J., Tian, M., Wu, L. Y., *et al*. (2020). Ten-Nanometer-Depth Lithium Niobate Nanostructures with Sub-Nanometer Surface Roughness. Journal of Micromechanics and Microengineering, 30(10), 105009.

[8] Hill, R., & Storåkers, B. A Concise Treatment of Axisymmetric Indentation in Elasticity. In: Eason, G., & Ogden, R.W. (Eds.). Elasticity: Mathematical Methods and Applications. Chichester: Ellis Horwood, 1990, pp. 199-210.

[9] Greenwood, J. A. (2010). Contact Between an Axisymmetric Indenter and a

Viscoelastic Half-Space. International Journal of Mechanical Sciences, 52(6), 829-835.

[10] Sneddon, I. N. (1946). Boussinesq Problem for a Flat-Ended Cylinder. Proceedings of the Cambridge Philosophical Society, 42(1), 29-39.

[11] Abbott, E. J., & Firestone, F. A. (1933). Specifying Surface Quality − A Method Based on Accurate Measurement and Comparison. Journal of Mechanical Engineering, 55, 569-572.

[12] Kanafi, M. M. (2020). Surface generator: artificial randomly rough surfaces (https://www.mathworks.com/matlabcentral/fileexchange/60817-surface-generator-artificial-randomly-rough-surfaces), MATLAB Central File Exchange. Retrieved September 30, 2020.

[13] McCool, J. I. (1986). Comparison of models for the contact of rough surfaces. Wear, 107(1), 37-60.